Zdeněk Matěj[a], Radomír Kužel[a], Milan Dopita[b], Miloš Janeček[c], Jakub Čížek[d], Tereza Brunátová[a]

[a] Department of Condensed Matter Physics, Charles University, Faculty of Mathematics and Physics, Praha, Czech Republic
[b] Institute of Materials Science, TU Bergakademie Freiberg, Freiberg, Germany
[c] Department of Physics of Materials, Charles University, Faculty of Mathematics and Physics, Praha, Czech Republic
[d] Department of Low Temperature Physics, Charles University, Faculty of Mathematics and Physics, Praha, Czech Republic

XRD profile analysis of ECAP Cu and Cu + Zr samples

Technical purity copper and copper with addition of 0.18 wt.% of zirconium samples processed by equal channel angular pressing with different number of passes were studied by X-ray line profile analysis. Dislocation-induced broadening is the dominant effect determining diffraction line shape. X-ray analysis reveals increasing mean dislocation density ($\sim 10^{15}\,m^{-2}$) with the number of ECAP passes. The character of the deformation field connected with the dislocation distribution is slightly different in pure copper than in copper with addition of zirconium and evolves significantly during 4 or 8 ECAP passes in the case of pure copper.

Keywords: Ultrafine-grained copper; ECAP; XRD; Dislocations

1. Introduction

Equal channel angular pressing (ECAP) is a severe plastic deformation (SPD) technique capable of producing fully dense and bulk submicrocrystalline and nanocrystalline materials [1]. Copper is a well-defined model material for the study of the SPD process. Its properties after treatment by many other methods have been studied for a long time. The microstructure of the samples of pure copper and copper with a small addition of zirconium processed by ECAP was characterised by positron annihilation spectroscopy (PAS), electron backscatter diffraction (EBSD), and X-ray diffraction (XRD). Results of XRD analysis are presented here; results of EBSD experiments are presented separately by Dopita [2]. XRD can be used to characterise various aspects of the sample microstructure [3], e. g.: texture, residual stress, crystallite size, character and density of defects, in particular dislocations. The aim of this study is to characterise dislocation densities and distribution in the mentioned Cu samples. Two approaches of XRD line profile analysis were used: the simplified method using peak profile parameters and total-pattern-fitting [4, 5].

2. Experimental procedure

Two series of samples were studied: technical purity (99.95 %) Cu and Cu with a small addition (0.18 wt.%) of Zr were deformed by ECAP to a maximum equivalent strain of 8 (1, 2, 4, and 8 passes) at room temperature following route B_c. The details of the die design as well as of the ECAP pressing are given elsewhere [6].

XRD data for line profile analysis were measured with the aid of Panalytical X'Pert Pro powder diffractometer in the symmetrical Bragg – Brentano geometry using filtered Cu-K_α-radiation and variable divergence and anti-scatter slits. A part of the measurements was performed with the PIXCel position-sensitive detector. The correction for instrumental broadening was performed with the aid of a NIST standard LaB_6. In the case of total-pattern-fitting the profile parameters describing angular dependency of width and shape of peaks of the LaB_6 sample were used to describe the instrumental function as in Ref. [4]. For data treatment based on extracting profile parameters of individual peaks two Pearson-VII functions (one describing the instrumental and the other the physical broadening) were numerically convoluted and then fitted to the measured data. This procedure is similar to that used by Scardi et al. [7], but here only the extracted parameters of the physical broadening component were subsequently analysed.

3. Results

Both used methods of XRD analysis are based on the model of dislocation-induced broadening developed by Wilkens [8]. The Wilkens model is widely described and explained, e. g. in Refs. [4, 5, 7 – 9]. It has two parameters: dislocation density ρ and the Wilkens characteristic parameter M describing in a simplified way the dislocation distribution. This parameter affects mainly the shape of diffraction peaks. When $M \gg 1$, the dislocation distribution is associated with long-range strain fields and the diffraction peaks are nearly Gaussian. Dislocations are distributed homogeneously if $M \sim 1$. Peak profiles with long tails of Lorentzian shape are associated with short-range strain fields and $M \ll 1$ (Fig. 1). Formulas derived by Wilkens [8] for the Fourier transformation of diffraction profiles can be found mainly in Refs. [4, 5, 7 – 9]. Line broadening associated with finite crystallite size is described by a model assuming spherical crystallites and the log – normal distribution of their diameter. Hence, the crystallite size is characterised by the median of this distribution M_D and the second parameter, σ, determining the shape of the size distribution [4, 5, 7].

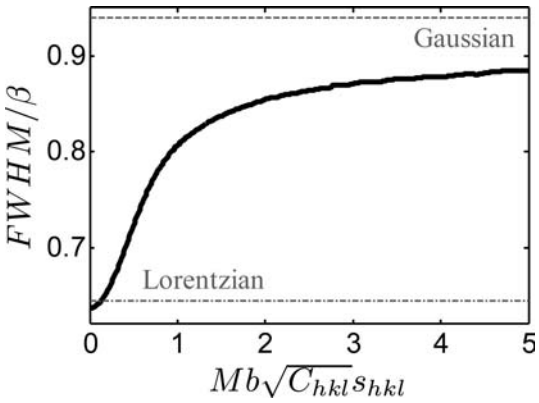

Fig. 1. *FWHM/β* ratio of the physical broadening component calculated numerically according to the Wilkens dislocation model [4, 5, 7–9] as a function of the scaling quantity ($MbC_{hkl}^{1/2}s_{hkl}$), where M is the Wilkens parameter, b is the Burgers vector, C_{hkl} is dislocation contrast factor and s_{hkl} is the diffraction vector length. If M is small, the profiles are more Lorentzian-, for high M values more Gaussian-like.

The first simplified approach used for data analysis is based on the treatment of profile parameters obtained by fitting of convoluted Pearson-VII functions to the measured data. Peaks have well defined shape with small negligible asymmetry (Asym = 1.00 +/−0.10). Small systematic line shifts, almost the same for all samples, were observed. They show a (*hkl*)-dependence characteristic for residual stresses as in the case of the Reuss model [3]. However, residual stress measurements did not reveal the presence of any significant stress. The total-pattern-fitting analysis including the effect of stacking faults, another possible origin of systematic line shifts and asymmetry, showed that the defect probability is lower than 0.5 %. The effect of line shifts is small. It does not affect the line profile analysis and was neglected. Two parameters were used for the profile analysis. The first was the full width at half of maximum (*FWHM*). Peak widths of all samples are only slightly different and show typical anisotropy of the type $FWHM_{h00} \gg FWHM_{hhh}$ (Fig. 2). This can be well explained by the orientation factors calculated assuming only dislocations with the Burgers vector $\boldsymbol{b}$ ||<110> that are typical for the fcc structure [4, 5] (Fig. 3). The *FWHM/β* ratio (Fig. 4) was chosen as the second parameter. Here $\beta = A/I_0$ is the profile integral width: the ratio of the profile integrated intensity A and the profile maximum value I_0. It is compared to the *FWHM* more sensitive to the profile tails. Diffraction peaks of the pure Cu sample after 8 ECAP passes are noticeably more Lorentzian-type than the peaks of all other samples (Fig. 4). *FWHM/β* ratios of samples with addition of Zr are in most cases slightly more Gaussian-type than *FWHM/β* ratios of pure Cu samples. More exact results were refined from these *FWHM* values and *FWHM/β* ratios by fitting them based on the Wilkens model and the size distribution model, which is the final step of the first approach.

The second approach used is the total-pattern-fitting [4, 5] making use of the same size and dislocation-broadening models. All the broadening effects were convoluted, the whole powder pattern was simulated and fitted to the measured data (Fig. 5). The second parameter of the size distribution model could also be refined in this analysis, but in order to simplify interpretation it was kept constant at the average value $\sigma = 0.4$. The modified program FOX [10] for microstructure analysis [11] was used. Refined parameters of the size and dislocation-broadening models are shown in Table 1. Mean dislocation density and Wilkens parameter obtained by the total-pattern-fitting are shown in Figs. 6, 7.

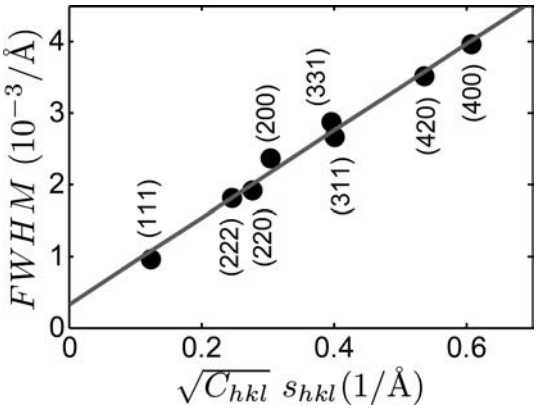

Fig. 3. *FWHM* values for the Cu-1 sample as a function of the diffraction vector length s_{hkl} scaled by the square root of the dislocation contrast factor C_{hkl} (modified Williamson–Hall plot).

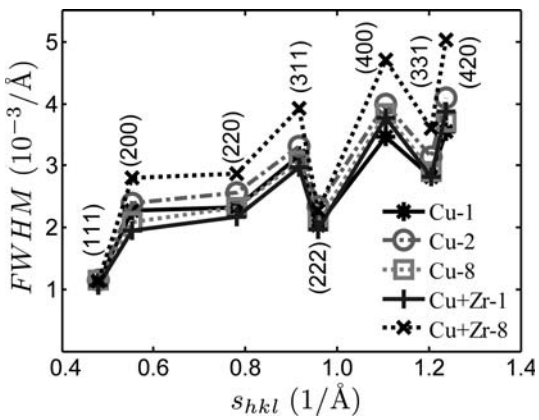

Fig. 2. *FWHM* values (Williamson–Hall plot) for some Cu and Cu + 0.18 % Zr samples (Cu-1: the pure Cu sample after 1 ECAP pass, Cu + Zr-8: the Cu + 0.18 % Zr sample after 8 ECAP passes, etc.). *FWHM* values show typical anisotropy for the dislocation-induced broadening. s_{hkl} is the diffraction vector length.

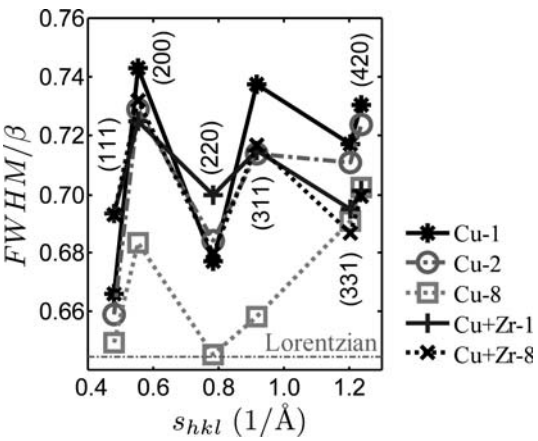

Fig. 4. Values of *FWHM/β* ratio determined by the Pearson-VII function fitting (for same samples as in Fig. 2). Diffraction profiles of the Cu-8 sample are clearly more Lorentzian-type than profiles of all other samples.

Table 1. Microstructure parameters for pure Cu and Cu + Zr samples treated by different number of ECAP passes (1, 2, 4, 8). Parameters were obtained by fitting peak profiles parameters (marked FWHM) and by the total-pattern-fitting (TPF): M_D – median of the crystallites size distribution, ρ – dislocation density, M – Wilkens parameter.

	$D_{M,FWHM}$ nm	$D_{M,TPF}$ nm	ρ_{FWHM} 10^{15} m^{-2}	ρ_{TPF} 10^{15} m^{-2}	M_{FWHM}	M_{TPF}
Cu-1	48 +/– 6	68.0 +/– 0.6	2.6 +/– 0.9	2.15 +/– 0.03	0.38 +/– 0.08	0.48 +/– 0.01
Cu-2	45 +/– 7	61.8 +/– 0.5	3.7 +/– 1.7	2.79 +/– 0.03	0.34 +/– 0.09	0.51 +/– 0.01
Cu-8	49 +/– 7	65.7 +/– 0.4	7.9 +/– 7.8	3.68 +/– 0.05	0.22 +/– 0.11	0.39 +/– 0.01
Cu + Zr-1	41 +/– 5	56.8 +/– 1.1	4.1 +/– 1.2	1.57 +/– 0.06	0.26 +/– 0.05	0.57 +/– 0.03
Cu + Zr-2	52 +/– 7	70.8 +/– 1.9	4.6 +/– 1.8	2.33 +/– 0.07	0.45 +/– 0.12	0.89 +/– 0.06
Cu + Zr-4	52 +/– 6	72.6 +/– 1.8	7.0 +/– 3.2	2.30 +/– 0.06	0.43 +/– 0.12	1.17 +/– 0.07
Cu + Zr-8	56 +/– 7	59.7 +/– 1.1	5.3 +/– 2.3	3.05 +/– 0.13	0.49 +/– 0.13	0.82 +/– 0.05

4. Discussion

There is a significant difference between refined values obtained by the two used methods of X-ray line profile analysis (Table 1), mainly concerning parameters of the dislocation-broadening model (the Wilkens parameter M and the dislocation density ρ). The more direct but simplified method is the first approach using the Pearson-VII function. It accounts properly for all effects, with one important simplification: a phenomenological function (Pearson-VII) is chosen to obtain only one shape parameter ($FWHM/\beta$) which is subsequently analysed. This is connected with two weak points of the method: the bias of the chosen profile function and the accuracy of the determined shape parameter ($FWHM/\beta$). The possibility to observe directly some trends of the extracted parameters ($FWHM$ and $FWHM/\beta$), e. g. the difference between Cu-8 and all other samples in Fig. 4, is the advantage of this approach. The total-pattern-fitting method consists of simultaneous modelling of the shapes of all diffraction lines in a complex way using physically relevant profiles based on the microstructure model. It is clearly a more sensitive technique compared to the first one. Both methods are based on the same microstructure model but they are treating data in a different way and hence result in refined microstructure parameters which are averaged differently. Deviations of the real sample microstructure from the simplified ideal model can result in different averaged microstructure parameters determined by these analysis techniques. This partially reveals shortcomings of the model. In spite of a good agreement of the measured and calculated powder patterns (Fig. 5) the model is not ideal. More real models of dislocation line-broadening with a reasonable number of parameters still have not been developed sufficiently. The methods using the width and shape parameters (e. g. the Williamson – Hall plot method) are advised usually only for studying trends, while complex modelling methods (total-pattern-fitting) are regarded as sufficiently robust to be suitable for quantitative microstructure analysis [12]. Hence also here the results of the total-pattern-fitting method were considered as more reliable. Moreover only the re-

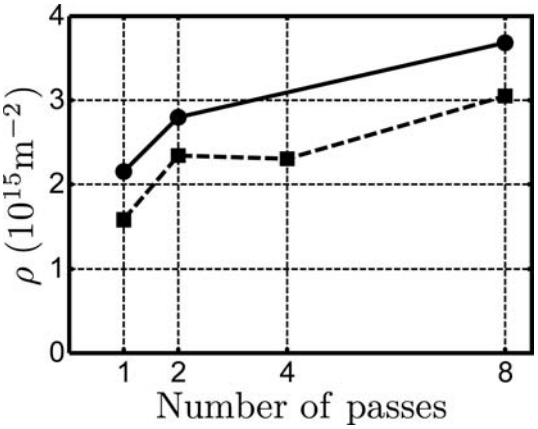

Fig. 6. Dependence of the mean dislocation density ρ obtained from the total-powder-pattern-fitting on the number of ECAP passes. ● pure Cu; ■ Cu + 0.18 % Zr.

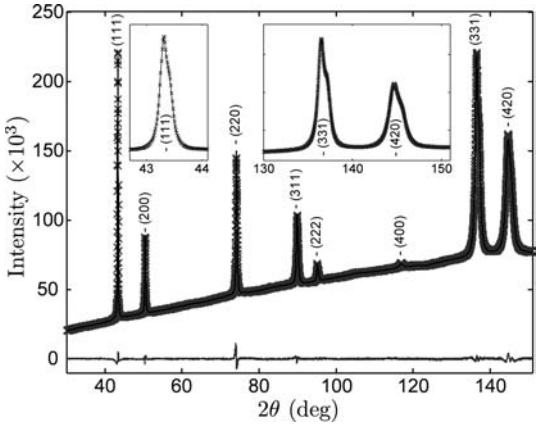

Fig. 5. Result of the total-pattern-fitting of the Cu-1 sample data (pure Cu after 1 ECAP pass). Gray (×) symbols: measured data; black full line: fit; gray full line: difference plot.

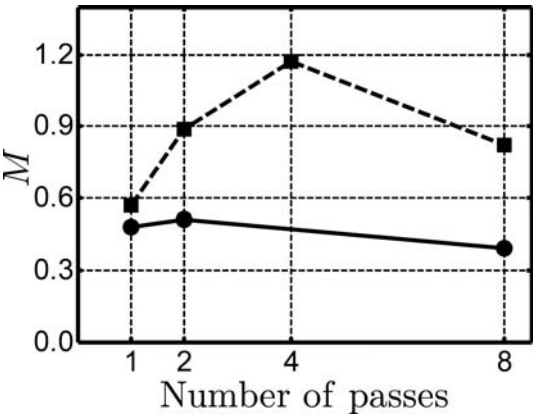

Fig. 7. Dependence of the Wilkens M parameter obtained from the total-powder-pattern-fitting on the number of ECAP passes. ● pure Cu; ■ Cu + 0.18 % Zr.

sults which show same trends as revealed by both methods were considered as finally reliable.

XRD analysis showed an increasing non-saturating mean dislocation density of absolute values higher than 10^{15} m^{-2}. Increasing dislocation density is in agreement with PAS experiments. However, absolute values cannot be compared because PAS reports saturated trapping and only a lower limit for dislocation density $>10^{14}$ m^{-2}.

The Wilkens dislocation parameter, M, reveals a decreasing trend in pure Cu samples treated by 4 or 8 ECAP passes (Table 1, Figs. 4, 7). This decrease was considered to be reliable because it is directly noticeable in the measured profile shapes and also shape parameters (Fig. 4). The M parameter for Cu + 0.18 % Zr shows in Fig. 7 a quite complex evolution with the number of passes. This trend of M values, refined by the total-pattern-fitting, is not in agreement with the trend of the M parameters determined by the direct method using shape parameters. Simulations showed that the differences between profiles with the Wilkens parameter $M \sim 0.8$ and $M \sim 1.2$ are small as compared by differences between profiles with $M \sim 0.4$ and $M \sim 0.8$. Hence it was concluded that the real uncertainty of values $M \sim 1$ is big and the differences between refined values for higher M could be insignificant. On the other hand generally slightly higher M values for all Cu + 0.18 % Zr samples as compared with pure Cu samples were confirmed by both methods. Hence, it indicates that the dislocation distribution in Cu + 0.18 % Zr samples is slightly more random and homogeneous as compared with pure Cu samples.

The crystallite size was similar for all samples (confirmed by both methods) – about 60 nm – quite different from the grain size observed by EBSD measurements [2]. The peak-size broadening caused by grains of few microns diameter (as determined by EBSD) could not be detected by XRD. Spatial steps of fractions of micrometer and misorientation angles limits of a few degrees are usually used in EBSD measurements and grain size-analysis. The high density of defects in the ECAP samples is connected with lattice deformations and distortions. Such lattice distortions can, on a scale of hundreds of nanometres, result in lattice incoherency as seen by X-ray diffraction and hence give much smaller coherently scattering domains.

5. Conclusion

XRD analysis of ECAP Cu and Cu + Zr samples showed a dislocation density of the order of 10^{15} m^{-2}, increasing slightly with the number of ECAP passes. Variations of the XRD line profile shapes indicate that the character of the strain field associated with the dislocation distribution in pure Cu and Cu + 0.18 % Zr samples is slightly different. Dislocation arrangement in Cu + 0.18 % Zr seems to be more random than in pure Cu samples. The character of the dislocation strain field also changed significantly after 4 or 8 ECAP passes in the case of pure Cu sample.

The authors acknowledge funding of the Ministry of Education of the Czech Republic through the research program MSM 0021620834 and by the grants KAN400720701, KAN300100801 and IAA101120803 of the Academy of Sciences of the Czech Republic. One of the authors (M.D.) acknowledges the financial support through the German Research Council (DFG) under the project # KL 1274/4-1.

References

[1] N.Q. Chinh, J. Gubicza, T.G. Langdon: J. Mater. Sci. 42 (2007) 1594.
[2] M. Dopita, M. Janeček, D. Rafaja, J. Uhlíř, Z. Matěj, R. Kužel: Int. J. Mat. Res. 100 (2009) 785.
[3] R.L. Snyder, J. Fiala, H.J. Bunge (Eds.): Defect and Microstructure Analysis by Diffraction, Oxford University Press (2000).
[4] P. Scardi, M. Leoni: Acta. Cryst. A 58 (2002) 190.
[5] G. Ribárik, T. Ungár, J. Gubicza: J. Appl. Cryst. 34 (2001) 669.
[6] M. Janeček, B. Hadzima, R.J. Hellmig, Y. Estrin: Metall. Mater. 43 (2005) 258.
[7] P. Scardi, M. Leoni, Y.H. Dong: Eur. Phys. J. B 18 (2000) 23.
[8] M. Wilkens: Krist. Tech. 11 (1976) 1159.
[9] E. Wu, E.M.A. Gray, E.H. Kisi: J. Appl. Cryst. 31 (1998) 356.
[10] V. Favre-Nicolin, R. Černý: J. Appl. Cryst. 35 (2002) 734.
[11] Z. Matěj, L. Nichtová, R. Kužel: Materials Structure CSCA 15 (2008) 46.
[12] P. Scardi, M. Leoni, R. Delhez: J. Appl. Cryst. 37 (2004) 381.

(Received August 25, 2008; accepted December 10, 2008)

Bibliography

DOI 10.3139/146.110112
Int. J. Mat. Res. (formerly Z. Metallkd.)
100 (2009) 6; page 880–883

ISSN 1862-5282

Correspondence address

Zdeněk Matěj
Ke Karlovu 5, 12116 Praha 2, Czech Republic
Tel.: +420 221 911 455
Fax: +420 224 911 061
E-mail: matej@karlov.mff.cuni.cz

You will find the article and additional material by entering the document number **MK110112** on our website at *www.ijmr.de*